3-D KNEE CARTILAGE SEGMENTATION USING A SMOOTHING B-SPLINE ACTIVE SURFACE

Xian Du, Jérôme Velut, Radu Bolbos, Olivier Beuf, Christophe Odet and Hugues Benoit-Cattin

CREATIS-LRMN, CNRS UMR 5220 Inserm U 630
Université Claude Bernard Lyon 1, INSA Lyon, Bât. B. Pascal, 69621 Villeurbanne, France

ABSTRACT

We present an adaptive solution for guinea pig knee cartilage segmentation using a 3-D smoothing B-Spline active surface. An adaptive parametric combination of edge-based forces and balloon force solves the problem of capture range of external forces. The comparison between the results of the experiments using this method and previous 3-D validated snake segmentation shows that the accuracy and robustness are improved.

Index Terms— *biomedical image processing, image segmentation, spline functions, MRI*

1. INTRODUCTION

This paper deals with the segmentation of 3D MRI images of small animal knee cartilage using snake based approach. The context of such a study is the validation of osteoarthritis drugs on small animal models such as guinea pig [7]. MRI has significant reproducibility to quantify and access the degenerations of cartilages given accurate segmentation. 3-D cartilage segmentation of MRI image on small animals is challenging due to the poor resolution and noises. It is more complex than segmenting human cartilage as the minimum cartilage thickness of small animal between femur and tibia is around 300 µm instead of a few mm, whereas the real image noise maintains at the same level.

Snake [1] was used in image segmentation with the evolution driven by internal forces and external forces. The internal forces regularize the surface of snake: extension and curvature of curves. External forces drive snake to reach the boundary of image, normally by using edge-image information. However, snake suffers two problems: Contour initialization and capture range of external forces. Using balloon force [2], the initial contour can be far from the desired boundary. It prevents the contour from shrinking and can push contour into boundary concavities, whereas it may be too strong and overwhelm the "weak" edge. Gradient Vector Flow (GVF) [3] makes use of the diffusion of the gradient vector of edge map to capture large range and concavity, whereas it is sensitive to noise and parameter. Vector Field Convolution (VFC) [4] convolves a vector field kernel with edge map to improve the robustness to noise and initialization, whereas it does not work well in homogeneous regions of the image. When applied to 3-D MRI image segmentation (especially on small animals), those methods were constrained largely by MRI image resolution, noise, manual interaction and 2-D based algorithms.

Prior knowledge has also been introduced to recover those missing cartilage boundaries. Active Shape Model [5, 6] enabled cartilage segmentation to be accurate and reproducible. However, those techniques require tedious training process and are only consistent with training data. In addition, those technologies were based on 2-D extension in essence.

We present a 3-D segmentation algorithm by introducing adaptive external forces to the 3-D smoothing B-Spline active surface (SBAS) [8] to improve the accuracy and robustness of the cartilage segmentation, which is applied and evaluated on real MRI image data of guinea pig. The bone cartilage interface (BCI) can be obtained accurately and quickly by this algorithm. Note that the minimal cartilage thickness is the target that will be found by determining the BCI of femur and tibia respectively and by finding in 3D the minimum distance between these two interfaces as detailed in [7].

The BCI segmentation process is described in the following. Firstly, for each MRI data, the initial snake for BCI will be the same which is set according to the shape and position of segmentation target. Such initialization results from the fact that small animals like guinea pig have similar features in their knees and cartilages in group. The central points of the volume data are assumed to be identical. Secondly, adaptive external forces which incorporates the relationship between evolution process and external force range, govern snake evolution.

The outline of the paper is as follows. In section II, we propose an adaptive and smoothing BCI segmentation method: The SBAS is introduced and an adaptive scaling of forces allows surface evolving process to be more accurate. In section III, our segmentation approach is validated by experiments on guinea pig cartilage segmentation and comparison with the 3-D segmentation of [7]. In section IV, we draw conclusion on the proposed method.

2. METHOD

2.1. Active surface framework

An evolving 2D snake is described by a curve $\vec{v}(s,t)=[x(s,t),y(s,t),z(s,t)]$ parameterized by arc length s, ($s\in[0,1]$) and depending on time *t*. The BCI 2D segmentation aims to obtain a curve that minimizes energy E_{snake} defined by:

$$E_{snake} = E_{int} + E_{ex} \qquad (Eq.\ 1)$$

This minimization can be solved by the corresponding Euler-Lagrange differential equation and a force balance equation is obtained as follows:

$$F_{int} + F_{ext} = 0 \qquad (Eq.\ 2)$$

In this model, F_{int} generally regularizes the extension and curvature of curves. F_{ext} is the sum of traditional potential forces, such as image forces, that attract snake to the contour of image. Meanwhile, the additional forces are generally introduced to increase the capture range of an active contour, such as balloon force, GVF, VFC and so on.

In [9], a smoothing B-spline filter SB_λ is introduced to control the curvature of a contour according to a parameter λ, instead of F_{int}. In [8], Velut et al. extended the Smoothing B-Spline snake to a Smoothing B-Spline Active Surface (SBAS), yielding a 3D segmentation method. The initial surface is a quadrangular mesh that is deformed using the snake framework of Figure 1. In this framework, the iterative deformation of each snake point is yielded as follows:

$$\hat{g}_{i+1}(k,l) = \hat{g}_i(k,l) - \gamma^{-1}.(sb_{\lambda,\mu} * f_i(k,l)) \qquad (Eq.\ 3)$$

where $\lambda=\mu$ is the regularization parameter, *i* is the iteration index, $\hat{g}_{i+1}(k,l)$ and $\hat{g}_i(k,l)$ are the regularized snake points *(k,l)* at iteration *i+1* and *i* respectively. $f_i(k,l)$ is the deformation vector generated by the sum of external forces at each snake point *(k,l)* and at each iteration *i*, γ is a step-size parameter involved in the speed of convergence, and $sb_{\lambda,\mu}(k)$ is the impulse response of the smoothing B-spline filter $SB_{\lambda,\mu}$.The regularization is controlled trough a unique parameter λ that tunes the cut-off frequency of the smoothing B-Spline filter used to smooth the deformation forces. Such algorithm provides a framework to integrate prior knowledge or local image information in B-snake.

2.2. Deformation forces definition and active control

For BCI segmentation, SBAS algorithm is applied with external forces defined by a combination of image force vectors (noted F_{image}) and balloon force (noted $F_{balloon}$):

$$\vec{F}_{ext} = \alpha.\vec{F}_{image} + \beta.\vec{F}_{balloon} \qquad (Eq.\ 4)$$

where α, β are weighting parameters that control the contribution of the above two forces respectively.

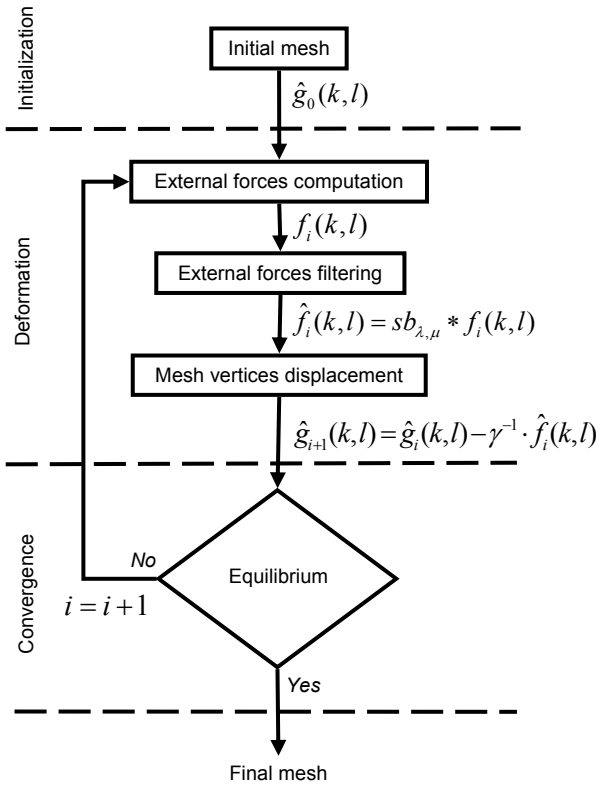

Figure 1: Smoothing B-Spline Snake algorithm.

In this paper, image force is defined by the Laplacian applied to the image that has first been smoothed with a Gaussian smoothing filter in order to reduce its sensitivity to noise. Hence, the image force and the corresponding external energy are described as follows:

$$F_{image} = -\nabla E_{ext}(x,y,z) \qquad (Eq.\ 5)$$

$$E_{ext}(x,y,z) = -\left|\nabla\left(G_\sigma(x,y,z) * I(x,y,z)\right)\right|^2 \qquad (Eq.\ 6)$$

where $G_\sigma(x,y,z)$ is a three-dimensional Gaussian function with standard deviation σ, ∇ is the gradient operator and *I(x,y,z)* is the image gray level locating at coordinate *(x,y,z)*.

Balloon force defined by Cohen et al. [2] acts in a direction normal to the curve. In such a scheme, it is tedious to define by trial and error an optimal scale combination of image force and balloon force. A simple factor selection can be:

$$\begin{aligned} \alpha &= c \\ \beta &= 1-\alpha \end{aligned} \qquad (Eq.\ 7)$$

where c is the constant of Eq. 3 locating between 0 and 1.

Using the settings of Eq. 7 can not guarantee that snake slows down its evolving step as it is very near or on the image boundary. We propose in Eq. 8 an adaptive scaling of these weighting parameters that improves the

robustness of snake evolution and avoid trial and error tuning of these parameters.

$$\alpha = c.IterationDone / NumberOfIterations$$
$$\beta = (1 - IterationDone / NumberOfIterations).(1 - c)$$
(Eq. 8)

where *NumberOfIterations* is the total iteration number to be done and *IterationDone* is the finished iteration number.

As shown in Figure 2, scale factors α (for image force) and β (for balloon force) would change with iteration numbers, which is different from [11] where the balloon force adapts spatially only. It follows the phenomenon in snake evolving: When initial snake starts running, the edge information is not enough, and balloon force should be stronger; when snake approaches image edge closely, balloon force should fade as edge-based forces become stronger.

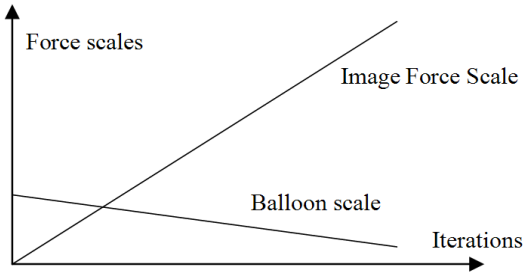

Figure 2: Scale factors of forces.

3. EXPERIMENTS AND RESULTS

3.1. MRI data set

We worked on the same MRI data set than in [7]. It has been obtained with a 7 T Biospec system (Brüker, Germany). A fat suppressed three-dimensional (3D) gradient-echo fast imaging (GEFI) sequence has been used with a flip angle α of 25°, TE=3.6 ms, TR=50 ms, and 42 kHz receiver bandwidth. A total of 64 slices (312 µm thick) was acquired in the sagittal plane with a field of view of 30 mm and an imaging matrix size of 512 x 384 pixels, corresponding to a reconstructed spatial resolution of 59 x 59 μm^2.

Finally, we applied the segmentation algorithm on a resliced volume of interest of 64^3 voxels with an isotropic resolution of 59 µm. We worked on two guinea pigs groups: SHAM with 9 animals used as control and MNX with 10 animals with meniscectomy.

3.2. Segmentation algorithm

The SBAS algorithm associated to the adaptive combination of deformation forces were implemented using VTK library and Python language on the MRI images data set. The process aims at the segmentation of femur bone cartilage interface (FBCI) and tibia bone cartilage interface (TBCI). The initial surfaces for FBCI and TBCI are quadrangular patches extracted from a sphere and a plane respectively (Figure 3).

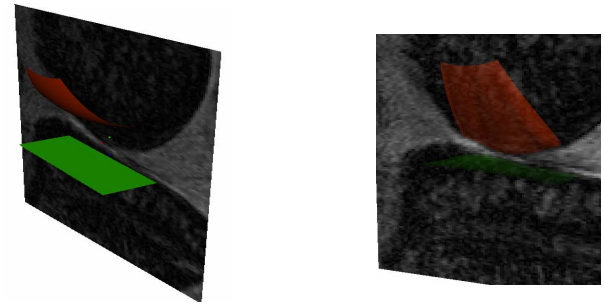

a) *b)*

Figure 3: Local segmentation of the FBCI (red) and the TBCI (green). a) Initialization with two quadrangular mesh patches. b) Final results.

We choose the smoothing regulator $\lambda = 500$ and iteration number N_1=*600* for FBCI and N_2=*300* for TBCI respectively.

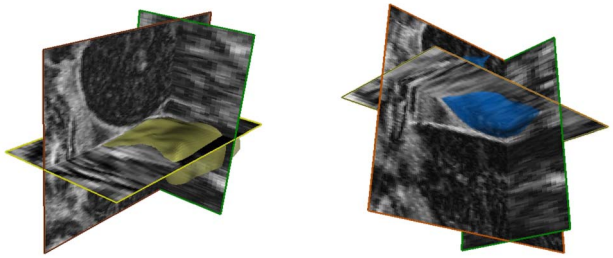

a)TBCI surface. *b)FBCI surface.*

Figure 4: Whole segmentation of tibia and femur BCI.

As illustrated in Figure 4, the proposed algorithm is able to segment the whole TBCI and FBCI and can be used to compute a thickness map of the cartilage (Figure 5). In order to conduct a quantitative assessment of the proposed algorithm similar to the one in [7], we consider only the central part of the cartilage (Figure 3).

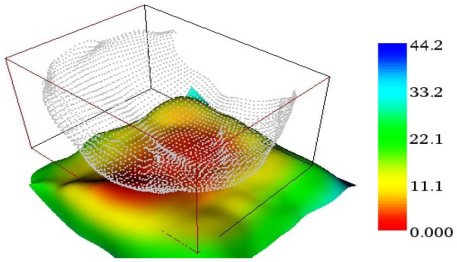

Figure 5: 3D map of the cartilage thickness.

3.3. Segmentation assessment

The quantitative segmentation assessment is based on the minimum cartilage thickness [7] that equals the minimum distance between the FBCI and TBCI. This parameter enables to compare the segmentation results quantitatively in terms of accuracy with histological results (HISTO)

working as reference and previous 3D snake based segmentation method (SOVITA) [7].

The segmentation results are analyzed for the two animal groups (SHAM and MNX) in terms of mean and standard error of mean (S.E.M) defined by:

$$SEM = \sigma / \sqrt{n} \qquad (Eq.\ 9)$$

where σ is the standard deviation of the minimum thickness and n is the number of images by group.

3.4. Results

The results are given in Table 1 for the two groups of data. The comparison shows the proposed method SBAS obtains more accurate measurement of the minimum thickness than the SOVITA one compared with the HISTO one.

The SEM behavior is similar in the two data groups. For both of these two groups, the SEM values are similar to those of SOVITA. The results indicate that the improvement of accuracy is obtained without losing the reproducibility of cartilage thickness measurement.

SHAM group	SBAS	HISTO	SOVITA [7]
No of samples	9	9	9
Min thickness average (μm)	324	329	314
S.E.M	8.2	4.7	8.5
MNX group	SBAS	HISTO	SOVITA [7]
No of samples	10	10	10
Min thickness average (μm)	310	317	294
S.E.M	13.3	4.5	12.4

Table 1: Segmentation results given as the minimum cartilage thickness on the two data groups (SHAM and MNX).The proposed approach (SBAS) is compared with a published approach (SOVITA) and histological data (HISTO).

The SBAS method simplifies the manual tuning of image force scale and balloon force scale with the integration of the two scales by using an adaptive parameter. In addition, with such a deformation force combination and proper selection of iteration number, initial surfaces are not limited by external force range due to different data set, which improves the robustness of segmentation.

4. CONCLUSIONS

This paper presents a 3D bone cartilage segmentation approach based on a SBAS coupled with an adaptive deformation forces combination. Such adaptive scheme facilitates the tuning of the segmentation algorithm and enhances the robustness of segmentation to initialization.

A quantitative assessment based on histological reference shows that the proposed approach improves the accuracy of the cartilage thickness measurements.

As illustrated in Figure 4, the proposed method is not limited to the measurement and analysis of cartilage thickness. Other criteria, such as cartilage volume, topography, articular contact areas, and surface feature can also be extracted from the quantitative analysis of the segmentation results.

ACKNOWLEDGEMENTS

MRI acquisition has been realized on ANIMAGE, the small animal imaging platform of Lyon, France. This project has been funded by the Institut de Recherches SERVIER. We thank the French CNRS for postdoc financial support of X. DU.

REFERENCES

[1] M. Kass et al., "Snakes: Active Contour Models", *International Journal of Computer vision*, pp. 321-331, 1988

[2] L. D. Cohen, "On active Contour Models and Balloons", *CVGIP: Image Understanding*, vol. 53, no 2, pp. 211-21, Mar. 1991.

[3] C. Xu and J. L. Prince, "Gradient Vector Flow: a new external force for snakes", *Proc. IEEE CVPR'97*, pp.66-71, 1997.

[4] Bing Li, "Vector field convolution for image segmentation using snakes", *Proc. IEEE ICIP'06,* pp 1637-1640, 2006.

[5] S. Solloway, C.E. Hutchinson, J.C. Waterton, C.J. Taylor, "The use of active shape models for making thickness measurements of articular cartilage from MR images", *Magnetic Resonance in Medicine*, vol. 37, no 6, pp. 943-952, 1997.

[6] J. Fripp, S. Crozier, S. Warfield, "Automatic Initialization of 3D Deformable Models for Cartilage Segmentation," *Proc. Digital Imaging Computing: Techniques and Applications*, pp. 513- 518, 2005.

[7] R. Bolbos et al., "Knee cartilage thickness measurements using MRI: a 4 1/2-month longitudinal study in the meniscectomized guinea pig model of OA", *Osteoarthritis and Cartilage*, vol. 15, no 6, pp. 656-665, June 2007.

[8] J. Velut, H. Benoit-Cattin, and C. Odet, "Segmentation by Smoothing B-Spline active surface". *Proc. IEEE ICIP'06*, pp. 209/-212, 2006.

[9] J. Velut, H. Benoit-Cattin, C. Odet, "Locally regularized smoothing B-Snake", *Journal on Advances in Signal Processing*, vol. 2007, ID 76241, pp. 12, 2007.

[10] J. A. Lynch, S. Zaim, J. Zhao, A. Stork, C.G. Peterfy, H. K. Genant, "Cartilage segmentation of 3D MRI scans of the osteoarthritic knee combining user knowledge and active contours", *Proc. SPIE.* vol. 3979, pp. 925-935, 2000.

[11] X. B. Li and J. K. Wang, "Adaptive balloon models", *IEEE Computer Society Conference on Computer Vision and Pattern Recognition (CVPR'99),* vol. 2, pp. 2434, 1999